Proposal for theoretical improvement of semi-physical forest fire spread models thanks to a multiphase approach

Proposal for Theoretical Improvement of Semi-Physical Forest Fire Spread Models Thanks to a Multiphase Approach: Application to a Fire Spread Model Across a Fuel Bed

Albert Simeoni * (1), Paul - Antoine Santoni (1), Michel Larini (2) and Jacques - Henri Balbi (1)

(1) SPE – CNRS URA 2053, Campus Grossetti, Università di Corsica,

(2) IUSTI – CNRS UMR 6595, Technopôle de Château-Gombert

ABSTRACT

This paper is devoted to the improvement of semi-physical fire spread models. In order to improve them, a theoretical approach based on the multiphase concept was carried out. The multiphase approach which considers the finest physical phenomena involved in fire behaviour was reduced by making several assumptions. This work led us to a simplified set of equations. Among these, a single equation for the thermal balance was obtained by using the thermal equilibrium hypothesis. This approach has been applied to the improvement of our semi-physical model in order to take into account increasing wind influence. The predictions of the improved model were then compared to experimental data obtained for fire spread conducted across pine needle fuel beds. To this end, different slope values and varying wind velocities were considered. The experimental tendency for the variation of the rate of spread was predicted. Indeed, it increases with increasing wind velocity for a given slope as well as for a given wind with increasing slope.

Keywords: Fire spread, multiphase flow, semi-physical models.

*e-mail: simeoni@univ-corse.fr, Tel: 00 (33) 4 95 45 01 61, Fax: 00 (33) 4 95 45 01 62

NOMENCLATURE

a	absorptivity
C_p	specific heat at constant pressure
e	total energy
$\vec{e}$	radiant intensity direction
$\vec{g}$	acceleration due to gravity
h	enthalpy
h^0	heat of formation
k	reduced heat transfer coefficient
k_v	reduced advection coefficient
k_v^*	constant in the k_v expression
K	thermal diffusivity
L	heat of vaporisation
L^Ω	radiant intensity
m	surface thermal mass
$\dot{M}$	mass flux
p	pressure
q	heat flux
Q	reduced combustion enthalpy
R	radiant flux
s	surface mass
t	time
T	temperature
u	internal energy

$\vec{V}$ velocity

$\vec{V}_{\infty}$ maximal wind velocity

w vertical component of the velocity

x, y, z coordinates of a point in space

Y mass fraction of a chemical species

Greek symbols

α volume fraction

β Stephan – Boltzmann constant

δ thickness of the fuel layer

γ combustion time constant

Γ rate of production of a chemical species at the solid / gas interface

ΔH reaction enthalpy of solid phases

ϕ flame tilt angle

λ_g thermal conductivity

$\vec{\nabla}_s$ surface divergence vector

$\dot{\omega}$ species mass rate of production

Ω solid angle

$\bar{\bar{\pi}}$ viscous stress tensor

$\bar{\bar{\Pi}}$ total stress tensor

ρ density

σ surface to volume ratio

θ angle located between the normal of the front and the direction of spread

Diacriticals

$[\ ]$	source term
$\bar{}$	average property over the fuel depth
$\|\ \|$	Euclidean value

Subscripts

a	ambient
g	gaseous phase
gk	interface exchanges
ig	ignition
k	a solid phase
s	surface component of a vector
sl	slope
w	wind
0	initial condition

superscripts

eq	medium equivalent to the litter
i	chemical species *i*
pr	gaseous products
surf	surface regression
δ	value at the surface of the bed

INTRODUCTION

Forest fire spread modelling involves several different approaches. According to the classification by Weber (1990), one can define three kinds of modelling. The simplest models are the statistical ones, which do not incorporate physical mechanisms (McArthur, 1966). There are also empirical models, (Rothermel, 1972) that are based upon the conservation of energy but these do not distinguish the modes of heat transfer. Finally, the physical models differentiate among the various kinds of heat transfer in order to predict fire behaviour (Albini, 1985 and Weber, 1991). Among these, multiphase modelling, which takes into account the finest physical phenomena involved in fire spread, represents the most complete approach to have been developed to date (Grishin, 1997 and Larini et al., 1997). The fuel and gaseous medium are represented as a multiphase medium. This formulation incorporates both the basic physical mechanisms and strong coupling between the phases due to mass and energy transfers. The solving of models based on this approach requires significant computer resources, however. This prevents them from being used as operational management tools for forest fighting at the present time. On the other hand, they can be regarded as an aid in improving the models devoted to the development of forest fire simulators.

The aim of our research team is to create an operational management tool able to describe the spread of a forest fire in order to help fire fighters make the appropriate decisions when dealing with multiple fires. It is therefore necessary to rapidly determine the approximate development of each fire involved. Thus, the simulator developed must be characterised by a short calculation time. This necessitates a simple model capable of predicting the key features of a fire. In a previous study (Balbi et al., 1999), we developed a two-dimensional fire spread model, which will be recalled for reasons of clarity. This last approach was inspired by a diffusion-reaction equation and allowed us to determine, from a single equation, the main

characteristics of a laboratory-scale litter fire under windless and slopeless conditions. This model and its evolutions can be classified as semi-physical ones. Indeed, the main heat transfers are differentiated in this formulation and the model's parameters, which are fuel dependent, are obtained from the fire behaviour dynamics. In a second study, this model was improved in order to include slope effects (Santoni et al., 1999 and Morandini et al., 1999). An attempt was then made to incorporate the influence of wind by assuming a similar effect of wind and slope due solely to radiating flame heat transfer (Morandini et al., 2000). Although this derived model was able to predict both strong slope and combined slope and low wind effects, it failed to describe fire behaviour at increasing wind velocity.

In the present work, we propose to use the multiphase concept to improve the semi-physical or semi-empirical models. The key concept of this process, which can be applied regardless of the semi-physical model considered, has been derived in this paper in order to improve our formulation. To this end, the model proposed by Larini et al. (1997) was reduced by making several assumptions to obtain a thermal balance that approaches our formulation. This last result was used to modify our semi-physical model in an effort to investigate the wind-aided fire spread configurations that have been poorly predicted up to now.

The first section recalls the multiphase concept and the set of obtained equations. Subsequently, the semi-physical model to be improved is described in the second section. The multiphase reduction is presented in the third section and, finally, the improvement of our semi-physical model using the previous reduction is proposed in the fourth part. The fifth section is devoted to the presentation of the experimental method that was used to validate the results of the improved model. The last section concerns the confrontation of the results of the improved model with experimental data and the discussion. To this end, different slope values and varying wind velocities are considered for fire spread conducted across a pine needle fuel bed.

THE MULTIPHASE MODEL

As the bases of this model have already been presented (Larini et al., 1997), only the essential information of this work is provided here. The aim of this approach is to represent the fire spread medium as being reactive and radiative multiphase. This medium is defined by the fluid phase and *N* solid phases. Each solid phase consists of a set of particles that possess the same geometry and thermochemical properties (cf. figure 1). It is possible to study forest fire behaviour at the particle scale. The resulting set of equations would not be of interest, however. This led us to define an elementary multiphase volume to carry out averaged properties of both the gaseous and solid phases. This last volume should be smaller than the scale of the phenomenon but greater than the size of the particle.

The entire set of multiphase equations governing the previous averaged properties is obtained in two steps. Firstly, point equations for the fluid and fuel phases, as well as the interface conditions, are established using Delaye's formulation (1976). Secondly, the set of obtained equations is space averaged applying Anderson and Jackson's approach (1967) to the multiphase medium. Finally, Larini et al. (1997) obtained the system of averaged equations presented hereafter. For reasons of clarity, no symbol indicating that the variables are volume averaged was added:

Gas phase

Mass equation

$$\frac{\partial}{\partial t}\left(\alpha_g \rho_g\right) + \vec{\nabla}.\left(\alpha_g \rho_g \vec{V}_g\right) = \sum_k \left[\dot{M}\right]_{gk} \tag{1}$$

Chemical species equation

$$\frac{\partial}{\partial t}\left(\alpha_g \rho_g Y_g^i\right) + \vec{\nabla}.\left(\alpha_g \rho_g Y_g^i \vec{V}_g\right) + \vec{\nabla}.\left(\alpha_g \rho_g Y_g^i \vec{V}_g^i\right) - \alpha_g \rho_g \dot{\omega}_g^i = \sum_k \left[\dot{M}\right]_{gk}^i \tag{2}$$

Momentum equation

$$\frac{\partial}{\partial t}\left(\alpha_g \rho_g \vec{V}_g\right) + \vec{\nabla}.\left(\alpha_g \rho_g \vec{V}_g \vec{V}_g\right) - \vec{\nabla}.\left(\alpha_g \overline{\overline{\pi}}_g\right) - \alpha_g \rho_g \vec{g} = \sum_k \left[\dot{M}\vec{V}\right]_{gk} + \sum_k \left[\vec{\Pi}\right]_{gk} \tag{3}$$

Total energy equation

$$\begin{aligned} &\frac{\partial}{\partial t}\left(\alpha_g \rho_g e_g\right) + \vec{\nabla}.\left(\alpha_g \rho_g e_g \vec{V}_g\right) + \vec{\nabla}.\left(\alpha_g \left(\vec{q}_g + \vec{R}_g\right)\right) - \vec{\nabla}.\left(\alpha_g \overline{\overline{\pi}}_g.\vec{V}_g\right) \\ &- \alpha_g \rho_g \vec{g}.\vec{V}_g = \sum_k \left[\dot{M}e\right]_{gk} - \sum_k \left[q\right]_{gk} - \sum_k \left[R\right]_{gk} + \sum_k \left[\vec{\Pi}.\vec{V}\right]_{gk} \end{aligned} \tag{4}$$

Solid Phase (*N* equations, one per *k* phase)

Mass equation

$$\frac{\partial}{\partial t}\left(\alpha_k \rho_k\right) = -\left[\dot{M}\right]_k^{surf} - \left[\dot{M}\right]_k^{pr} \tag{5}$$

Chemical species equation

$$\frac{\partial}{\partial t}\left(\alpha_k \rho_k Y_k^i\right) = -\left[\dot{M}\right]_k^{surf,i} - \left[\Gamma\right]_k^{surf,i} - \left[\dot{M}\right]_k^{pr,i} \tag{6}$$

No momentum equation (motionless phase assumption)

Total energy equation

$$\frac{\partial}{\partial t}\left(\alpha_k \rho_k e_k\right) = -\left[\dot{M}e\right]_k^{surf} - \left[\dot{M}e\right]_k^{pr} - \left[q\right]_k - \left[R\right]_k + \left[\vec{\Pi}.\vec{V}\right]_k^{pr} \tag{7}$$

Interface equations (*N* equations)

Mass

$$\left[\dot{M}\right]_{gk} = \left[\dot{M}\right]_k^{surf} + \left[\dot{M}\right]_k^{pr} \tag{8}$$

Species

$$\left[\dot{M}\right]_{gk}^i = \left[\dot{M}\right]_k^{surf,i} + \left[\Gamma\right]_k^{surf,i} + \left[\dot{M}\right]_k^{pr,i} \tag{9}$$

No momentum interface equation (motionless solid phases)

Energy

$$\left[\dot{M}e\right]_{gk} - \left[q\right]_{gk} - \left[R\right]_{gk} + \left[\vec{\Pi}.\vec{V}\right]_{gk} = \left[\dot{M}e\right]_{k}^{surf} + \left[\dot{M}e\right]_{k}^{pr} + \left[q\right]_{k} + \left[R\right]_{k} - \left[\vec{\Pi}.\vec{V}\right]_{k}^{pr} \quad (10)$$

Radiative transfer equation

$$\vec{e}.\vec{\nabla}\left(\alpha_g L_g^{\Omega}\right) = \alpha_g a_g \left(\frac{\beta T_g^4}{\pi} - L_g^{\Omega}\right) + \sum_k \left[\frac{\alpha_k \sigma_k}{4}\left(\frac{\beta T_k^4}{\pi} - L_g^{\Omega}\right)\right] \quad (11)$$

The radiating flux present in the gas phase energy equation is determined from the radiative transfer equation using the following relation:

$$\vec{R}_g = \int_{\Omega} L_g^{\Omega}\, \vec{e}\, d\Omega \quad (12)$$

The radiative and convective flux into the solid phases are not taken into account as we consider the solid phases to be thermally thin and media opaque to radiation. It should be noted that the volume averaged form of the equations presented here were obtained by setting the assumption of correlation between all the variables equal to one. This important assumption simplifies the resolution of the whole multiphase system. From this method, different sub-models appear on the right side of the previous balance equations that need to be determined. These are not detailed here as they will not be used in the following sections, but the interested reader is referred to Larini et al. (1997). This approach will be used to propose a method for improvement of semi-physical forest fire spread models. For reasons of clarity we will present hereafter our semi-physical model, in which we will apply this method.

THE SEMI-PHYSICAL MODEL

The aim of our research team is to develop a simple fire spread model to be used within an operational management tool. Due to the amount of physical phenomena and state variables involved in fire behaviour, it is necessary to make some simplifying hypotheses in order to

generate a comprehensive and simple model. These hypotheses lead us to combine these physical phenomena and to consider a thermal balance that provides the framework of the model. We proposed a reaction-diffusion formulation which includes a cooling convective term so as to model fire spread. In order to write a thermal balance, elementary cells composed of soil and plant matter are defined. As a whole, these cells are considered to represent a thin, isotropic and homogenous medium equivalent to the litter. The energy transferred from a cell to the surrounding air is considered to be proportional to the difference between the temperature of a cell and the ambient temperature. Combustion reaction is assumed to occur above a threshold temperature (T_{ig}). Above this threshold, the fuel mass decreases exponentially and the quantity of heat generated per unit fuel mass is constant. The heat transferred between a cell and its neighbouring cells is due to three mechanisms: radiation, convection and conduction. We assumed that these exchanges can be represented by a single equivalent diffusion term, under no slope and no wind condition. However, due to obvious geometric reasons, a supplementary radiation was considered for up-slope fire (Santoni et al., 1999). For down-slope and no-slope fires, flames are tilted backwards and no supplementary radiant contribution from the flame is taken into account. The following hypotheses were proposed in order to evaluate the supplementary radiant contribution for upslope fires:

- We consider the flame to be a vertical radiant surface (cf. figure 2.a) at least up to a limit angle (Drysdale, 1992).
- We assume that the radiant heat flux prevails over a short distance d (in the calculation performed here, d is equal to the spatial increment value of 0.01 m).
- We consider that the flame temperature T is equal to the temperature of the burning cell located below it. This temperature is given by the model. By using a Stefan-Boltzmann law, we assume that the radiant heat flux is proportional to T^4.

These hypotheses allowed us to determine the supplementary radiant contribution (Santoni et al., 1999). From this last analysis, it was determined that an unburned cell in the direction of the slope receives an additional radiant heat flux from a burning cell directly before it, this additional heat flux being proportional to the cosine of the angle θ located between the normal of the front and the direction of the slope. Hence, when all of the previous assumptions are considered, we obtain the following radiant contribution in our model that can be viewed as a source term:

$$R = P(\phi_{sl})\cos(\theta)T^4(x-d,y,t) \tag{13}$$

Where $T(x-d,y,t)$ is the temperature of the burning cell located before the unburned cell under consideration, with P being a function of the slope angle.

Finally, we obtain the following model of fire spread:

$$\begin{array}{ll}
\dfrac{\partial T}{\partial t} = -k(T-T_a) + K\Delta T - Q\dfrac{\partial s_k}{\partial t} + R & \text{on the fuel complex} \\
R = 0, \quad s_k = s_{k0}e^{-\gamma(t-t_{ig})} & \text{for a burning cell} \\
R = P(\phi_{sl})\cos(\theta)T^4(x-d,y,t), \quad s_k = s_{k0} & \text{for an inert cell ahead of the fire front} \\
R = 0, \quad s_k = s_{k0} & \text{for an unburned cell elsewhere} \\
T = T_a & \text{at the boundaries far from the fire} \\
T(x,y,t=0) = T_a & \text{for an unignited cell at time zero} \\
T(x,y,t=0) = T_{ig} & \text{for an ignited cell at time zero}
\end{array} \tag{14}$$

where t_{ig} is the time at which $T = T_{ig}$.

The model parameters (k, K, Q and γ) are determined using the experimental temperature measurements over time for a fire spreading in a linear manner (Balbi et al., 1999). Due to our approach, these parameters are fuel-dependent and must therefore be identified for each fuel type. Thus, the usual fuel descriptors such as mass per unit area, particle size, compactness, physico-chemical properties and moisture content are intrinsically taken into account. The parameter P is a function of the flame tilt angle under up-slope conditions ϕ_{sl} and is determined for each slope in accordance with the rate of spread. It should be noted that the

flame tilt angle under slope conditions, ϕ_{sl}, is equal to the slope angle since we consider the flame to be a vertical radiant surface (cf. figure 2.a). For horizontal and down-slope fires, the flame leans backward and $P(\phi_{sl}) = 0$, which means that there is no supplementary radiant effect. For up-slope fires, an important increase in $P(\phi_{sl})$ is expected and Morandini et al. (2000) determined that a power sine law describes such variations:

$$P(\phi_{sl}) = p_0 \sin^4(\phi_{sl}) \tag{15}$$

where p_0 is a power sine law constant, the value of which will be provided later. Based on the laboratory fire experiments of Mendes-Lopes et al. (1998), an analogy was drawn between fire behaviour under slope conditions and its behaviour under wind conditions when flame tilt angle is below a threshold value (Morandini et al., 2000). Indeed, in these two cases, the rate of spread and flame behaviour are similar. This allows us to assume that the same dominant heat transfer mechanism, *i.e.* radiation, occurs in both cases. Therefore, wind effects were taken into account in the present model by means of the following radiant contribution (which is analogous to the one considered for slope effects):

$$R = P(\phi_w)\cos(\theta)T^4(x-d, y, t) \tag{16}$$

where ϕ_w represents the flame tilt angle under wind conditions (cf. figure 2.b), and the other terms are as described above. This model, which we can forthwith call the radiative model, remained valid for a combined slope and low wind velocity $(\leq 1 m s^{-1})$, but was not able to predict the fire behaviour under higher wind velocities (Morandini et al., 2000). In order to improve it, we propose to use the multiphase approach. However, this last approach is not suitable in its present form as it is too far removed from our semi-physical formulation.

We will thus reduce it in the next section in order to establish a comparison between our semi-physical model and the resulting multiphase reduced equations.

The multiphase model reduction is performed in three steps. Firstly, as the semi-physical model is two-dimensional, we have to *reduce* the three dimensional multiphase set of equations to two dimensions (cf. figure 3). Secondly, since the semi-physical and the semi-empirical models are generally characterised by a single energy conservation equation, the thermal balances of the multiphase model will be *reduced* to a single equation. Finally, the resulting conservation equation of energy is written in terms of temperature by using the previous set of reduced equations. This last result will be used to improve our semi-physical model.

For reasons of clarity, the three steps are only described below for the equations of energy, although this first step was applied to the entire set of multiphase equations.

Reduction to 2 dimensions

Eqs. 4 and 7 are averaged over the height δ by using the following operator, which allows us to be in agreement with the hypothesis of a medium equivalent to the litter, as defined in the semi-physical model:

$$\bar{f}(x,y,t) = \frac{1}{\delta}\int_0^{\delta} f(x,y,z,t)dz \tag{17}$$

A crucial point consists in determining δ. Should it be defined, for example, as being equal to the height of the flame, the scale of certain phenomena will not be respected (such as the flow in the fuel layer). Also, the mean value of the state variables would not vary enough to enable propagation. A solution consists in considering the thickness of the fuel layer. However, the phenomena occurring above this layer (for instance the flame radiation) are

taken into account by way of the boundary conditions at δ, which appear when managing the average operation.

The resulting equation is then simplified further to approach the semi-physical formulation. To this end, we make the following assumptions:

- Pressure, stress, gravity and conduction contributions are neglected in the gas phase,
- the state variable values at δ are considered equal to their mean values inside the fuel bed,
- the correlation equal to unity between all the variables is considered (such as for the space average procedure).

Thus, we obtain the following equations of energy:

$$\frac{\partial}{\partial t}\left(\overline{\alpha_g}\,\overline{\rho_g}\,\overline{u_g}\right)+\vec{\nabla}_s.\left(\overline{\alpha_g}\,\overline{\rho_g}\,\overline{u_g}\,\overline{\vec{V}_{g,s}}\right)+\frac{\left[\alpha_g\rho_g u_g w_g\right]_0^\delta}{\delta}+\vec{\nabla}_s.\left(\overline{\alpha_g}\,\overline{\vec{R}_{g,s}}\right)+\frac{\left[\alpha_g R_{g,z}\right]_0^\delta}{\delta}= \sum_k\left[\overline{\dot{M}h}\right]_{gk}-\sum_k\left[\overline{q}\right]_{gk}-\sum_k\left[\overline{R}\right]_{gk} \tag{18}$$

$$\frac{\partial}{\partial t}\left(\overline{\alpha_k}\,\overline{\rho_k}\,\overline{u_k}\right)=-\left[\overline{\dot{M}h}\right]_k^{surf}-\left[\overline{\dot{M}h}\right]_k^{pr}-\left[\overline{q}\right]_k-\left[\overline{R}\right]_k \tag{19}$$

These equations are expressed in terms of internal energy by subtraction of the kinetic energy balance. The right hand sides of Eqs. 18 and 19 are expressed in enthalpy. This is motivated by the need to set the equations in a form that enables resolution. Indeed, the formulation in enthalpy permits to link these expressions to sub models that need to be properly defined (cf. Larini, 1997 and Grishin, 1997).

Reduction to a single energy equation

In order to obtain a single equation, the equation of conservation of energy for both the fluid phase (Eq. 18) and *N* solid phases (Eq. 19) are added.

Thanks to the interface relation, (Eq.10), the right hand side of the obtained equation is equal to zero:

$$\frac{\partial}{\partial t}\left(\alpha_g \rho_g u_g\right) + \vec{\nabla}_s.\left(\alpha_g \rho_g u_g \vec{V}_{g,s}\right) + \frac{\left[\alpha_g \rho_g u_g w_g\right]_0^\delta}{\delta} + \vec{\nabla}_s.\left(\alpha_g \vec{R}_{g,s}\right) + \frac{\left[\alpha_g R_{g,z}\right]_0^\delta}{\delta} + \sum_k \frac{\partial}{\partial t}\left(\alpha_k \rho_k u_k\right) = 0 \quad (20)$$

For reasons of clarity, we have omitted the sign of averaged values along δ.

Temperature balance

The modification of Eq. 20 is achieved in two steps. First, we transform the internal energy into enthalpy by setting the following relation for each phase:

$$h_m = u_m + \frac{p_m}{\rho_m} \quad (21)$$

Then, we express the obtained equation in terms of temperature using the following relation and by assuming a constant heat capacity with temperature for each chemical species *i*:

$$h^i = C_p^i\left(T - T_0\right) + h^{i,0} \quad (22)$$

$h^{i,0}$ being the formation enthalpy at temperature T_0.

To further simplify the obtained equation, we make the following assumptions:

- A single solid phase is considered,
- thermal equilibrium between gas and solid phase inside the bed is assumed.

The assumption of thermal equilibrium between the two phases has already been made in both physical models (Grishin, 1997) and semi-physical models (Balbi et al., 1999). It has been verified in certain configurations and particularly in the pyrolysis zone. This is a very useful assumption, as it allows a description of propagation without going into description of the finer mechanisms that occur.

Finally, we obtain the following thermal balance:

$$\left(\alpha_g \rho_g C_{p,g} + \alpha_k \rho_k C_{p,k}\right)\frac{\partial T}{\partial t} + \alpha_g \rho_g C_{p,g} \vec{V}_{g,s}.\vec{\nabla}_s T + \vec{\nabla}_s.\left(\alpha_g \vec{R}_{g,s}\right) + \frac{\left[\alpha_g R_{g,z}\right]_0^\delta}{\delta} = -\left[\dot{M}\right]_k^{pr} L^{pr} - \left[\dot{M}\right]_k^{surf} \Delta H^{surf} - \sum_i \alpha_g \rho_g \dot{\omega}_i h_g^i \quad (23)$$

The terms located on the right hand side of this equation appear during the two operations of transformation (Eqs. 21 and 22), and particularly during the second step (Eq. 22), which permits to set the reaction terms. This equation represents the mean mechanisms of propagation, such as convection, radiation and reactions. Furthermore, it is expressed in a form that enables resolution through the expression of appropriate sub-models. It should be borne in mind that Eq. 23 is only a part of the whole reduced multiphase model derived from Eqs. 1 to 11. Thus, this reduced model remains too far from our aim, which is to elaborate a simple model capable of being used within an operating management tool. Eq. 23 will be compared hereafter with the semi-physical model (Eq.14) in an effort to improve it.

IMPROVEMENT OF OUR SEMI-PHYSICAL MODEL OF FIRE SPREAD ACROSS A FUEL BED

At this point, it should be recalled that the aim of this paper is to propose a theoretical method to improve semi-physical models. In the previous section, the reduction was carried out to obtain a formulation similar to our model. It is possible to reduce the complete multiphase set of Eqs. 1 to 11 differently in order to approach other kinds of semi-physical models. Here, we propose an application to our reaction-diffusion formulation in order to improve it. Indeed, Eq. 14 has been shown to poorly predict wind-aided fire behaviour across a fuel bed for wind velocities higher than $1\, m\, s^{-1}$.

By comparing Eq. 14 to Eq. 23, we can see that the essential aspects of fire spread behaviour are represented, with the exception of one such aspect in Eq. 14. Indeed, both

models consider chemical kinetics, radiant and convective heat transfer. The main difference between the two formulations consists in the advection contribution, which was omitted in our model:

$$\alpha_g \rho_g C_{p,g} \vec{V}_{g,s} . \vec{\nabla}_s T \tag{24}$$

Hence, we propose to add this term to the semi-physical model (Eq. 14), which thus becomes:

$$\frac{\partial T}{\partial t} + k_v \vec{V}_g . \vec{\nabla} T = -k(T - T_a) + K\Delta T - Q\frac{\partial \sigma_v}{\partial t} + R, \tag{25}$$

The added term should be discussed in order to identify the adequate values for the gas velocity $\vec{V}_g$ and coefficient k_v. With regards to $\vec{V}_g$, we assume that the maximum wind velocity $\vec{V}_\infty$ can be used in Eq. 25 to roughly take into account wind influence on propagation. Although we know that a boundary layer exists in the vicinity of the litter and that the velocity inside the fuel bed is not constant, we believe that the considered value for $\vec{V}_\infty$ will be a relevant approximation for the scale of the experiments under consideration. The form of coefficient k_v needs to be fully described. Indeed, it is derived from $\frac{\alpha_g \rho_g C_{p,g}}{\alpha_g \rho_g C_{p,g} + \alpha_k \rho_k C_{p,k}}$, which is obtained from Eq. 23.

This last ratio was transformed so as to be in accordance with our semi-physical approach. Thus, we obtained:

$$k_v = \frac{\alpha_g \rho_g \delta C_{p,g}}{m_{eq}} \tag{26}$$

where m_{eq} is the surface thermal mass of the semi-physical medium equivalent to the litter.

To calculate k_v, the following hypotheses are set:

- The specific heat of the gas mixture, $C_{p,g} = \sum_i C_p^i Y_g^i$, is taken as constant and equal to $1360\, J\, kg^{-1}$,
- α_g, the porosity of the multiphase medium, which is 0.97 for pine needles, is assumed to be constant (and equal to unity),
- m_{eq} is taken as constant according to Balbi et al. (1999),
- the gas mixture is taken as a perfect gas and we further assume that the quasi-isobaric approximation is valid.

Finally, we obtain the following expression for k_v:

$$k_v = \frac{\alpha_g \rho_a \delta C_{p,g}}{m_{eq}} \cdot \frac{T_a}{T} = k_v^* \cdot \frac{T_a}{T} \tag{27}$$

According to our previous hypotheses, k_v^* is a constant and k_v is only a function of temperature.

The improved model will be tested against experimental data for wind-aided fire spread across a fuel bed of pine needles, the data being obtained as described below.

EXPERIMENTAL FACILITY AND PROCEDURE

Experimental set-up

The experiments were carried out in a low speed wind tunnel, as depicted in figure 4, at the *Instituto Superior Técnico* of Lisboa (Mendes-Lopes et al., 1998). They were performed in order to observe wind driven fire across fuel beds of pine needles. Furthermore, the tunnel allows slope effects to be examined thanks to a sloping fuel tray.

The wind speed values range from –3 $m\, s^{-1}$ to 3 $m\, s^{-1}$. The movable tray can be set at angles from *0* up to *15*° with up-slope and down-slope orientation. The fuel bed occupies the

central part of the tray (*0.70 m* wide). It consists of a layer of *Pinus pinaster* needles and tries to reproduce a typical layer found in Portuguese stands, with a load of approximately *0.5 kg* m^{-2} on a dry weight basis and a fuel moisture content of (*10* ± *1%*).

Experimental runs

The movable tray is positioned at the required angle and the wind velocity is fixed at the required value. The conditioned pine needles are scattered uniformly on the tray. To insure a fast and linear ignition, a small amount of alcohol and a flame torch are used. The fuel is ignited at the wind tunnel end for wind driven fire, and at the opposite end for back-wind fires. In order to obtain a uniform and established flame propagation, ignition occurs at an appropriate distance from the work section. Three runs are carried out for each set of conditions. The experimental runs are video recorded.

Rate of spread, flame geometry and temperature recording

The rate of spread is obtained from the derivative of the curve *"flame front position vs time"*. Twenty to thirty images of each experimental run are analysed in order to determine the mean flame angle, which is defined as the angle between the tray and the leading surface of the flame. Temperature measurements are made using K type thermocouples with *250 μm* wire diameter.

NUMERICAL RESULTS AND DISCUSSION

Previous results (Radiative model)

Firstly, the varying experimental configurations were simulated using the semi-physical model (Eq. 14) proposed by Morandini et al. (2000). The model's dynamical coefficients

were determined thanks to experimental temperature curves under slopeless and windless conditions, as described in Balbi et al. (1999). We therefore obtain the following values:

$$k = 97\times10^{-3}\ s^{-1},\ K = 14.5\times10^{-6}\ m^2\ s^{-1},\ Q = 3.67\times10^{3}\ m^2\ K\ kg^{-1},\ \gamma = 0.234\ s^{-1},$$

$$p_0 = 9\times10^{-9}\ K^{-3}\ s^{-1} \qquad (28)$$

The predicted and observed temperature profiles are provided in figure 5. An overall similarity is observed for the shape of these simulated and experimental curves. The results have already been discussed in Balbi et al. (1999) and are not further described here.

The simulated rates of spread are provided in figures 6 to 8 for 0°, 5° and 10° upslope fires for wind velocities ranging from 0 to $3 m s^{-1}$. The results were in agreement with the experimental data up to a wind velocity of $1 m s^{-1}$. The model was not able to accurately describe the increase in the rate of spread with increasing wind velocities, however. Furthermore, the simulated values were significantly lower at the highest wind velocity of $3\ m s^{-1}$ than the experimental results.

Contribution of the improved semi-physical model

Different configurations were simulated for the range of slopes previously described and for wind velocities $\left\|\vec{V}_\infty\right\|$ of 1, 2 and 3 $m\ s^{-1}$, in order to compare the predictions of the improved and radiative models.

The value of k_v depends on the ratio k_v^*, which is a constant according to our hypotheses (cf. Eq. 27). We obtained the mean value $k_v^* \approx 7.5\times10^{-3}$. In light of the assumptions made to obtain relation 26 and the uncertainties in the variable values in the above ratio, the value of k_v^* given here should only be considered as an approximate result. In figures 6 to 8, which represent the rate of spread under varying configurations, two values of this coefficient have

been considered in the simulation, these values corresponding to $k_v \approx 7.5\times10^{-3} \pm 50\%$. Indeed, these values allow us to obtain a range for the experimental rates of spread. The lowest value of $k_v^* = 4\times10^{-3}$ is first used for all the configurations depicted in figures 6 to 8. With this value, we observe a good agreement between the predicted and observed fire speed for all of the slopes considered when the wind velocity is lower than or equal to 2 $m\,s^{-1}$. A substantial improvement is thus obtained over the previous radiative model, which, we recall, was not able to depict this tendency accurately. Indeed, the results of the improved model are nearer to those observed. Moreover, it more accurately predicts the fire rate of spread, which increases with increasing wind for a given slope. Nevertheless, the simulated results are not in agreement with the experimental data for a wind velocity value of 3 $m\,s^{-1}$, and this over the whole range of slopes considered (figures 6 to 8). Thus, even though progress has been made in comparison with the results of the radiative model, certain problems remain. At this stage, we used another value of $k_v^* = 11\times10^{-3}$, which leads to a significant improvement for the prediction of the rate of spread under wind velocities of 3 $m\,s^{-1}$. With regard to wind velocities of 1 and 2 $m\,s^{-1}$ (cf. figures 6 to 8), this value of k_v^* overpredicts the experimental data. Nevertheless, the general tendency for the rate of spread, which increases with increasing wind, is also provided. The reason behind this overprediction is to be found in the strong approximation made when considering the maximum wind velocity $\vec{V}_\infty$ in Eq. 23 instead of the gas velocity $\vec{V}_g$, which is not constant throughout the burning zone.

The multiphase approach can provide the gas velocity in the flaming zone. This last model requires that the whole range of Eqs. 1 to 11 be solved, however. This is not in accordance with the aim of our semi-physical approach, which is to elaborate a simple and robust model useful in management. In order to reach our goal, we will use here a simple wind profile in the burning zone to model the $\vec{V}_g$ variations, while keeping $k_v^* = 11\times10^{-3}$. Due to the

experimental configuration (cf. figure 4), we only consider $V_{g,x}$, the x component of $\vec{V}_g$ in Eq. 25. To obtain our profile, we assume that it is equal to $\left\|\vec{V}_\infty\right\|$ before entering the burning zone $\left(T = 300°C\right)$, and that it decreases to zero continuously in this area. To reproduce this behaviour, we have obtained a relation giving the profile of $V_{g,x}$, as a function of $\left\|\vec{V}_\infty\right\|$ and x, that is inspired by the study of the multiphase reduced model's flow equations. We have not developed this study here as this is beyond the scope of the present work and will be the object of another paper.

Figure 9 provides the simulated results, under no slope conditions and for varying winds, using the wind profile. We can observe an overall agreement between predicted and observed rates of spread, even if the model underpredicts fire spread for the highest velocity of 3 $m\ s^{-1}$. The difference between the simulated and experimental rates of spread for this high wind value can be explained by comparing the observed and predicted temperature profiles versus time at a given point (cf. figure 10). Before discussing these curves, it should be pointed out that the experimental temperature profiles can only be considered qualitatively, as mentioned by Ventura et al (1998). Nevertheless, three regimes can be defined that are more visible in the increasing slope configurations than in the no slope ones: preheating, peak temperature and cooling zones. That is why we present here the figure 10 for a 10° upslope fire. We can observe that the envelope of the simulated result roughly matches the experimental one. Discussion of the peak temperature zone is problematic as the thermocouples do not describe this zone accurately. Indeed, infrared measurements of the same fuel type (cf. Den Breejen, 1998) reveal that the burning area temperature ranges from 1000°C to 1300°C, which is in agreement with our predictions. The cooling in the third zone is observed although it cannot be analysed accurately due to differences in the performance of thermocouples in the same configurations (see also figure 5). As for the preheating zone, the model fails to qualitatively

describe the increase in fuel bed temperature (and this for all of the experimental runs considered). The reason for this is to be found in the radiant contribution modelling in Eq. 14. Indeed, in order to provide a simple model, we have assumed a short radiant distance effect by considering that radiation prevails in the inert cell ahead of the fire front. It is clear that this model can be further improved by taking into account the long distance effect of radiant heating ahead of the fire front. Thus, the under-prediction in the rate of spread for wind velocities of $3 m s^{-1}$ is a result of the modelling approach, and will be improved based on our theoretical multiphase investigation in future studies.

Moreover, two modelling aspects of our semi-physical formulation need to be discussed:

- The addition of the advection term in Eq. 25 implies that the fire can theoretically spread faster than the wind. The weak value of the constant $k_v^* = 11 \times 10^{-3}$ prevents us from reaching this condition since $k_v \leq k_v^* << 1$ (cf. Eqs. 25 and 27).
- The hypothesis of the thermal equilibrium between the gas and solid phase was not accurately verified by multiphase numerical investigations, as described by Porterie et al. (1998). For the experiments considered in the present study, this hypothesis has not been rejected, however. Nevertheless, it is possible that experimental configurations will reveal the necessity to model the gas phase temperature and the solid phase separately, in much the same way as we have demonstrated that advection was missing in our previous radiative model.

CONCLUSIONS

The present work was devoted to the use of the multiphase formulation as a tool to improve semi-physical models. To this end, a reduced model has been developed based on the

multiphase approach which has revealed a flaw in our semi-physical model: it was not able to take advection into account. We have therefore added a term representing this phenomenon in our formulation. We can assert that this addition has greatly improved the model, as it allowed us to generate a semi-physical two-dimensional fire spread model including both wind and slope conditions that is now capable of predicting rates of spread and temperature distributions for the main experimental conditions considered here. In order to continue this work, the wind profiles obtained by studying the flow equations of the reduced multiphase model will be presented in a subsequent paper.

Moreover, this study permits to theoretically link the semi-physical models to the more complete models by reducing the latter model type. The semi-physical models, whose aim it is to take into account the fine mechanisms involved in fire behaviour in a simple manner, require a way of developing simplified equations. We have shown in this paper that the reduced multiphase model has proved to be a relevant tool in the improvement of our formulation. It could be applied to other semi-physical and simple physical models devoted to developing operational management tools.

Another point which deserves mention is that our model is also capable of describing the front geometry, since it is two-dimensional along the fuel bed. This has been validated for both slopeless and slope configurations, although this was not possible for wind-driven spreading as we do not possess the contours for the experiments considered here. Further experiments are therefore necessary to definitively validate this.

Finally, in an effort to continue with the improvement of our semi-physical model, we will use the current theoretical approach in future studies to compare the other terms of our model with the reduced multiphase ones. In particular, the radiative term which remains oversimplified in the present model, will be examined.

REFERENCES

Albini, F.A. (1985) A model for fire spread in wildland fuels by radiation. *Combust. Sci. Tech.,* **42**, pp. 229-258.

Anderson, T. B. and Jackson, R. (1967) A fluid mechanical description of fluidized beds. *Ind. Engn. Chem. Fund.*, **6**, pp. 527-539.

Balbi, J. H., Santoni, P. A. and Dupuy, J.L. (1999) Dynamic modeling of fire spread across a fuel bed. *Int. J. of Wildland Fire*, (in press).

Delhaye, J.M. (1976) Local instantaneous equations – instantaneous space – averaged equations – two-phases flow and heat transfer. *Proceedings of NATO Advanced Study Institute*, **1**, Istambul.

Den Breejen, E., Roos, M., Schutte, K., De Vries, J. S. and Winkel, H. (1998) Infrared measurements of energy release and flame temperatures of forest fires. *III Int. Conf. on Fire Research,* **1**, pp. 517-532, Luso.

Drysdale, D. D., Macmillan, A. J. R. (1992) Flame Spread on Inclined Surfaces. *Fire Safety Journal*, **18**, pp. 245-254.

Grishin, A.M. (1997) In Albini (Ed.). *Mathematical modeling of forest fires and new methods of fighting them*. Publishing house of the Tomsk state university. Chap. 1. pp. 81-91.

Larini, M., Giroux F., Porterie B., and Loraud J.C. (1997) A multiphase formulation for fire propagation in heterogeneous combustible media. *Int. J. of Heat and Mass Transfer,* **41** (6-7), pp. 881-897.

McArthur, A.G. (1966) Weather and grassland fire behaviour. *Australian Forest and Timber Bureau Leaflet* N° 100.

Mendes-Lopes, J.M., Ventura, J.M., and Amaral, J.M. (1998) Rate of spread and flame characteristics in a bed of pine needles. *III Int. Conf. on Fire Research,* **1**, pp. 497-511, Luso.

Morandini, F., Santoni, P.A. and Balbi J.H. (1999) Validation study of a two-dimensionnal model of fire spread across fuel bed. *Comb. Sci. And Technology*, (in press).

Morandini, F., Santoni, P.A., and Balbi, J.H. (2000) Analogy between wind and slope effects on fire spread across a fuel bed – Modelling and validations. *3rd International Seminar on Fire and explosion hazards*. Lake Windermere, 10 – 14 April.

Porterie, B., Morvan, D., Loraud, J.C. and Larini, M. (1998) A multiphase model for predicting line fire propagation. *III Int. Conf. on Fire Research,* **1**, pp. 343-360, Luso.

Rothermel, R.C. (1972) A mathematical model for predicting fire spread in wildland fuels. *United States Department of Agriculture, Forest Service Research*. Paper INT-115. 40 pages.

Santoni, P. A., Balbi, J. H. and Dupuy, J.L. (1999) Dynamic modelling of upslope fire growth. *Int. J. of Wildland Fire*, (in press).

Ventura, J. M., Mendes-Lopes, J. M. and Ripado, L.M. (1998) Temperature-time curves in fire propagating in beds of pine needles. *III Int. Conf. on Fire Research,* **1**, pp. 699-711, Luso.

Weber, R.O. (1990) Modelling fire spread through fuel beds. *Progress in Energy and Combustion Science* **17**, pp. 67-82.

Weber, R.O. (1991) Toward a comprehensive wildfire spread model. *Int. J. of Wildland Fire,* **1** (4), pp 245-248.

(Page 7)

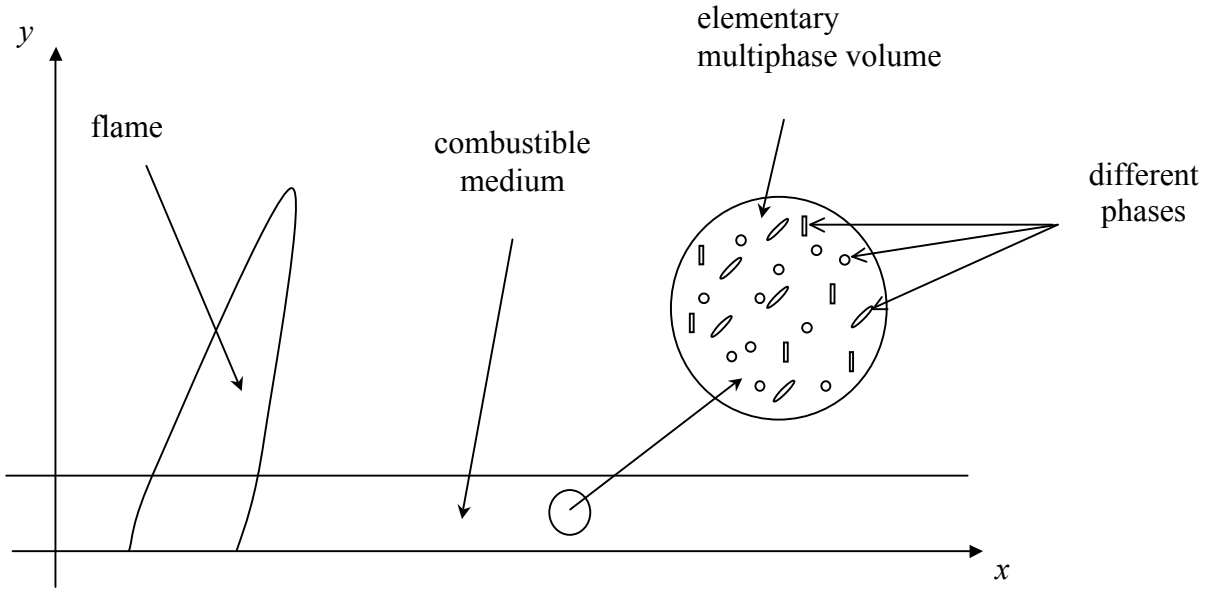

Figure 1: Schematic representation of the physical problem

(Page 10)

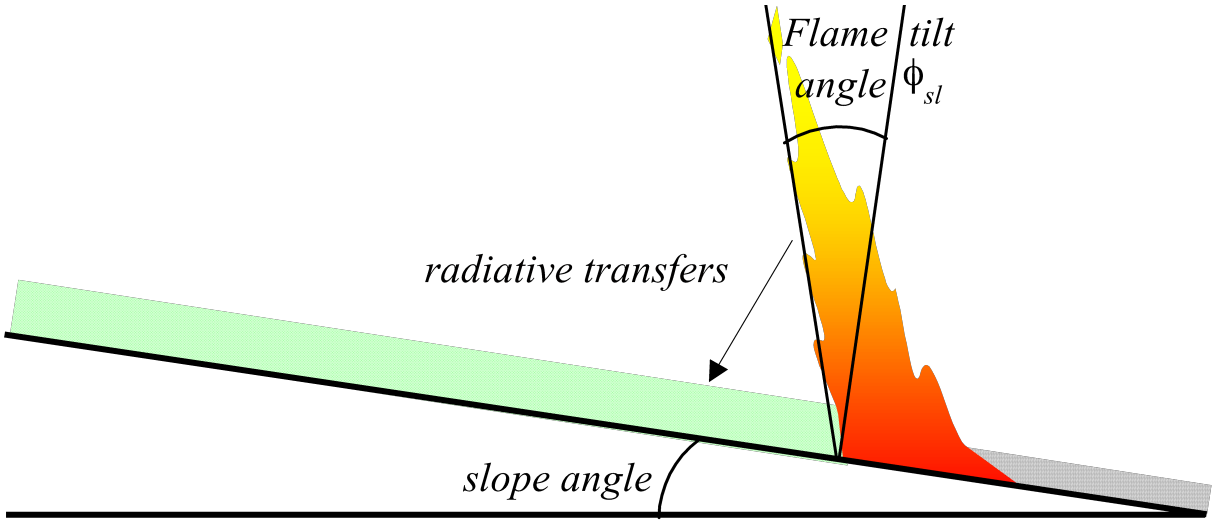

Figure 2.a: Flame tilt angle under slope condition

(Page 12)

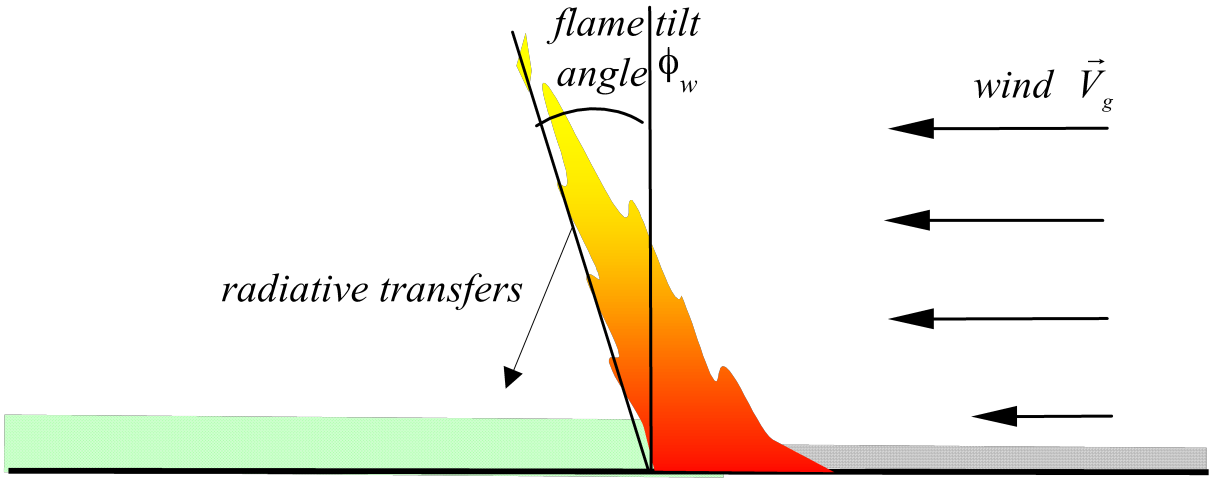

Figure 2.b: Flame tilt angle under wind condition

(Page 13)

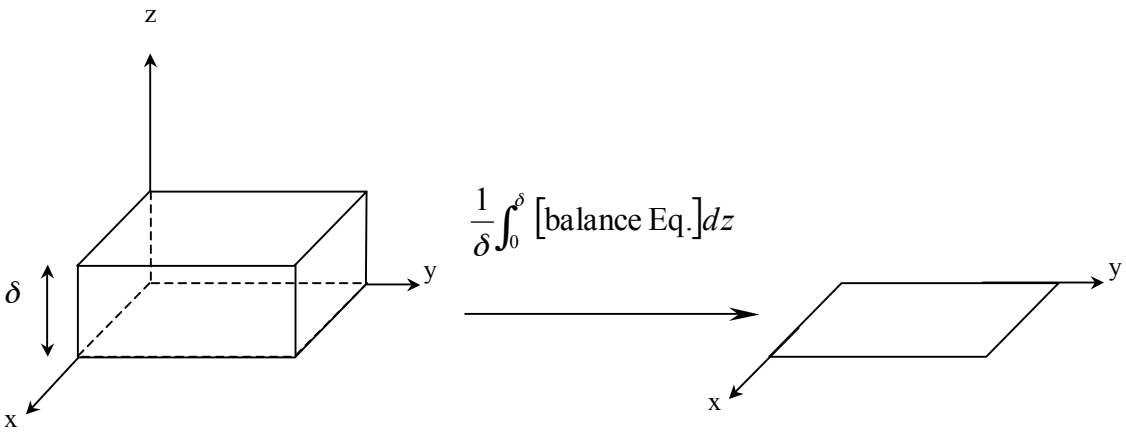

Figure 3: Two dimensional reduction procedure

(Page 18)

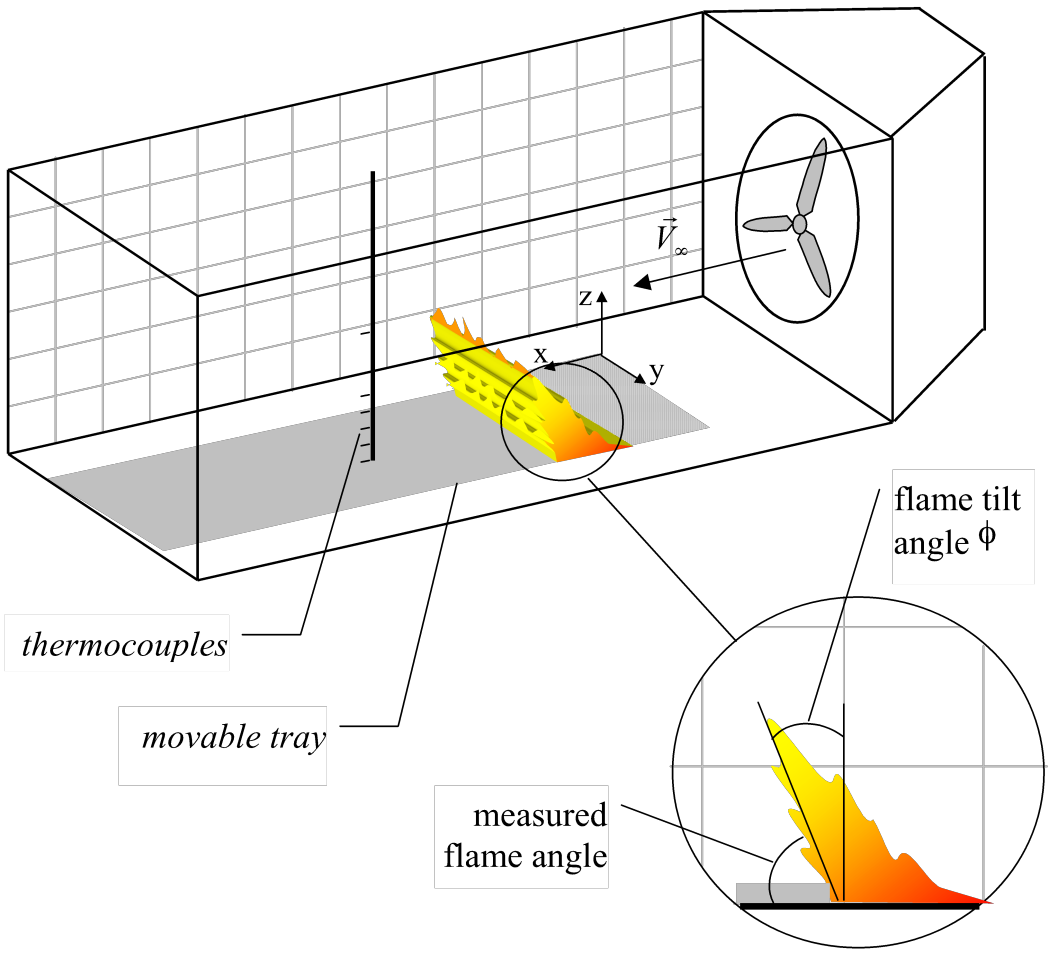

Figure 4: Experimental wind tunnel

(Page 19)

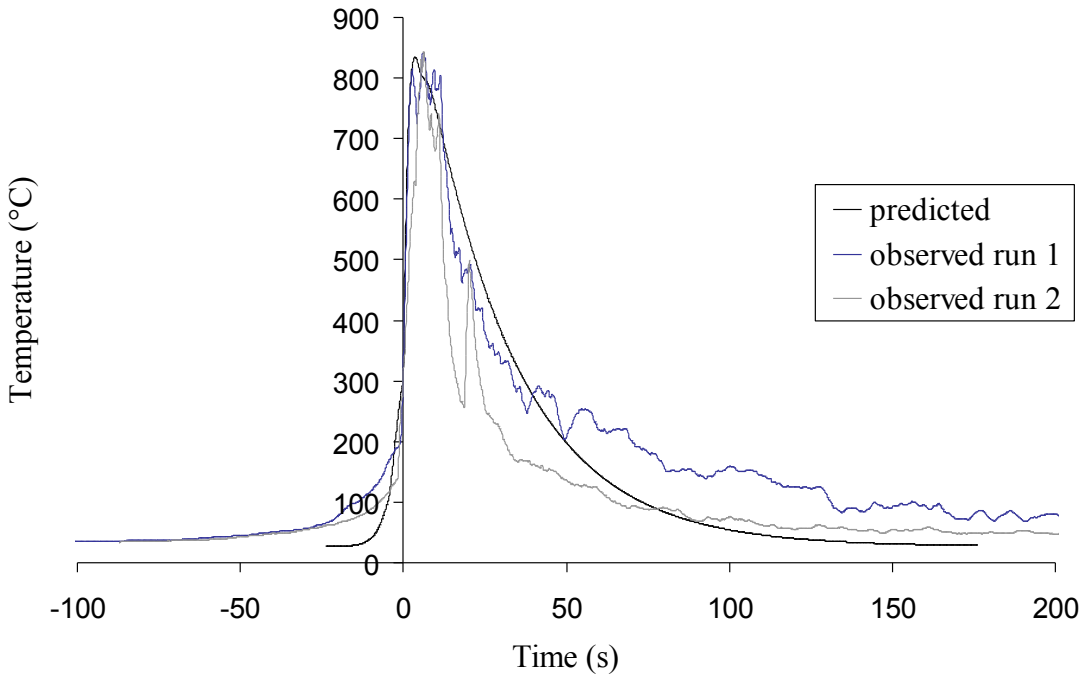

Figure 5: Experimental and predicted temperature curves

in slopeless and windless condition

(Page 20)

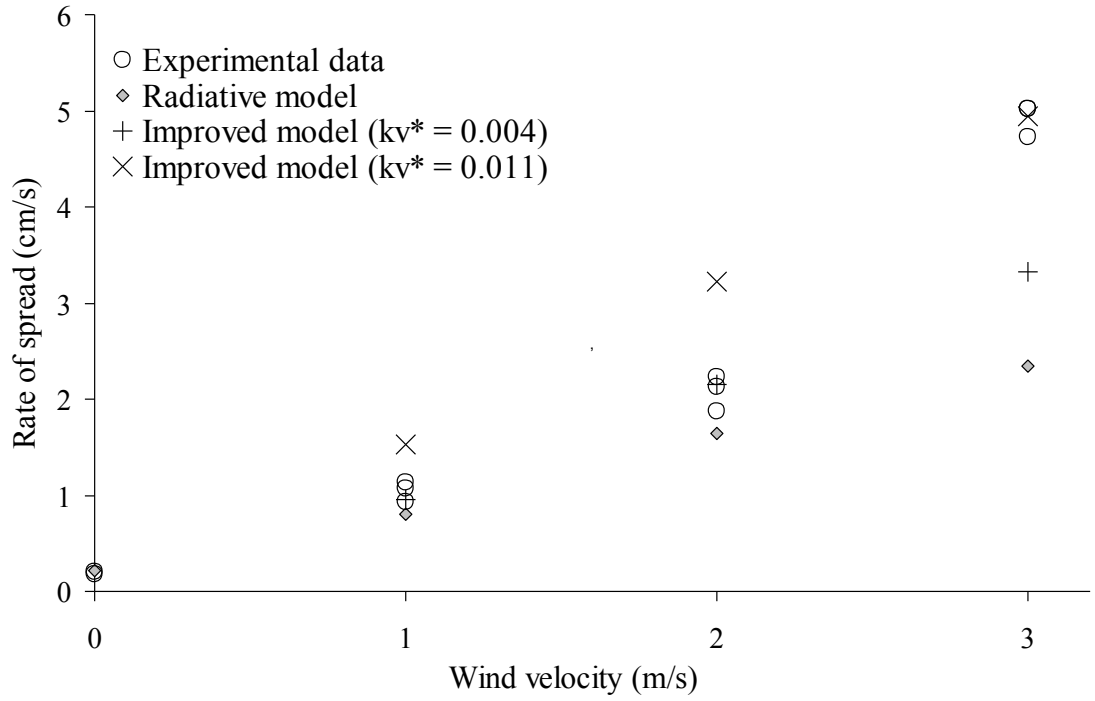

Figure 6: Rates of spread of the radiative and the improved model for no slope under various wind conditions

(Page 20)

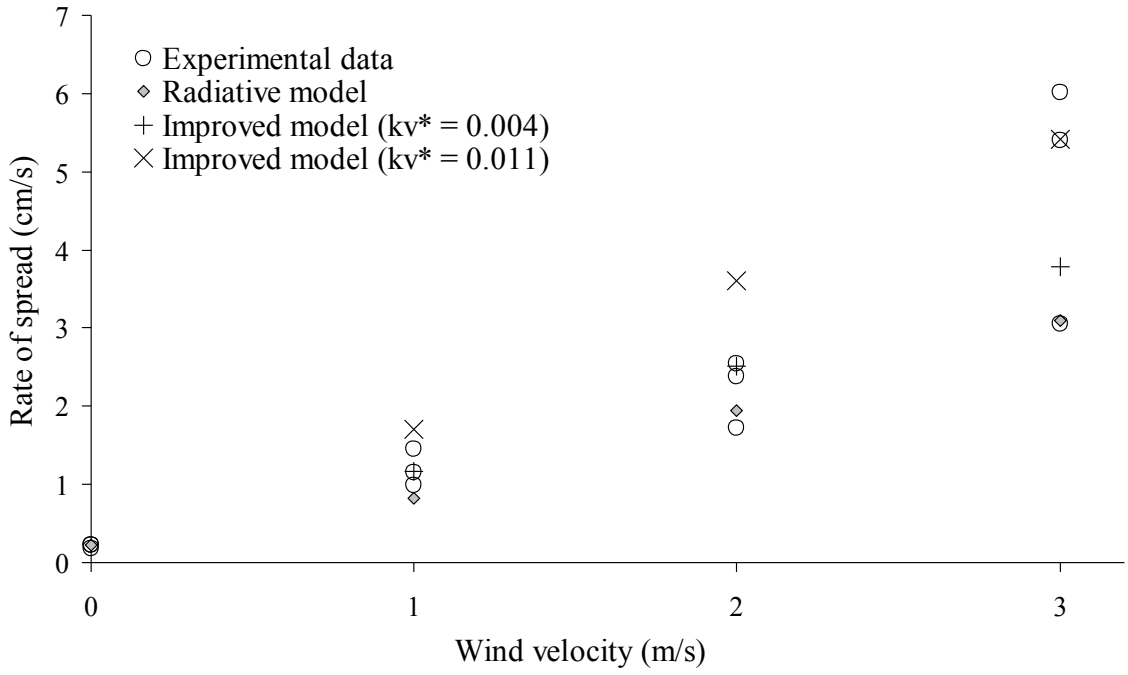

Figure 7: Rates of spread of the radiative and the improved model for a slope of 5° under various wind conditions

(Page 20)

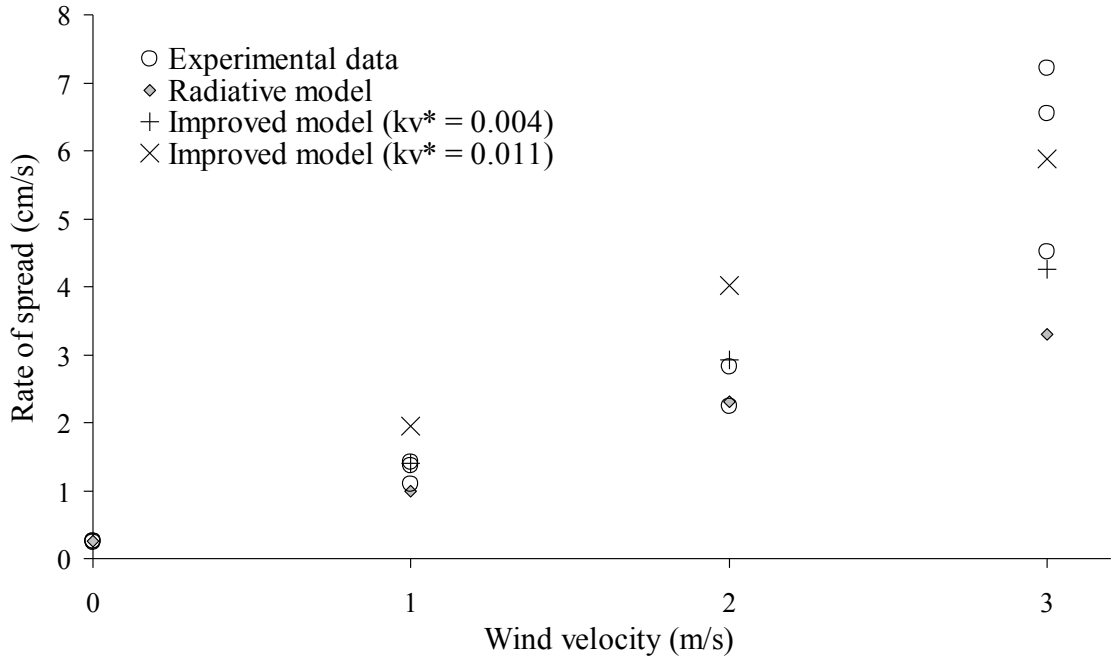

Figure 8: Rates of spread of the radiative and the improved model for a slope of 10° under various wind conditions

(Page 22)

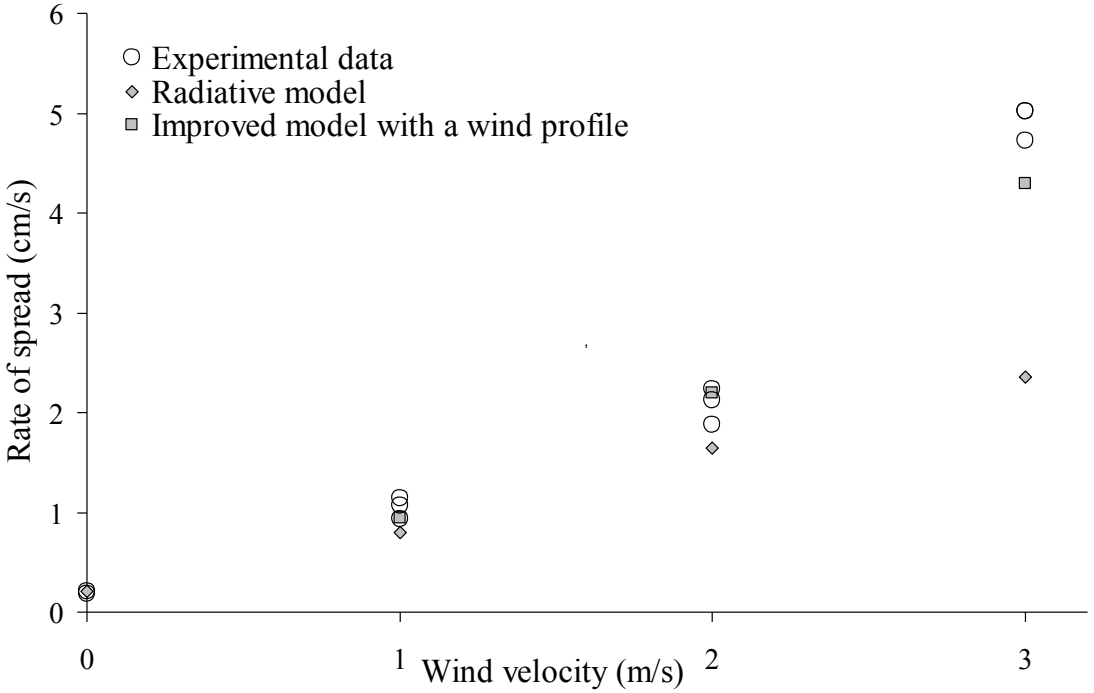

Figure 9: Rates of spread of the improved model including a wind profile for no slope and under various wind conditions

(Page 22)

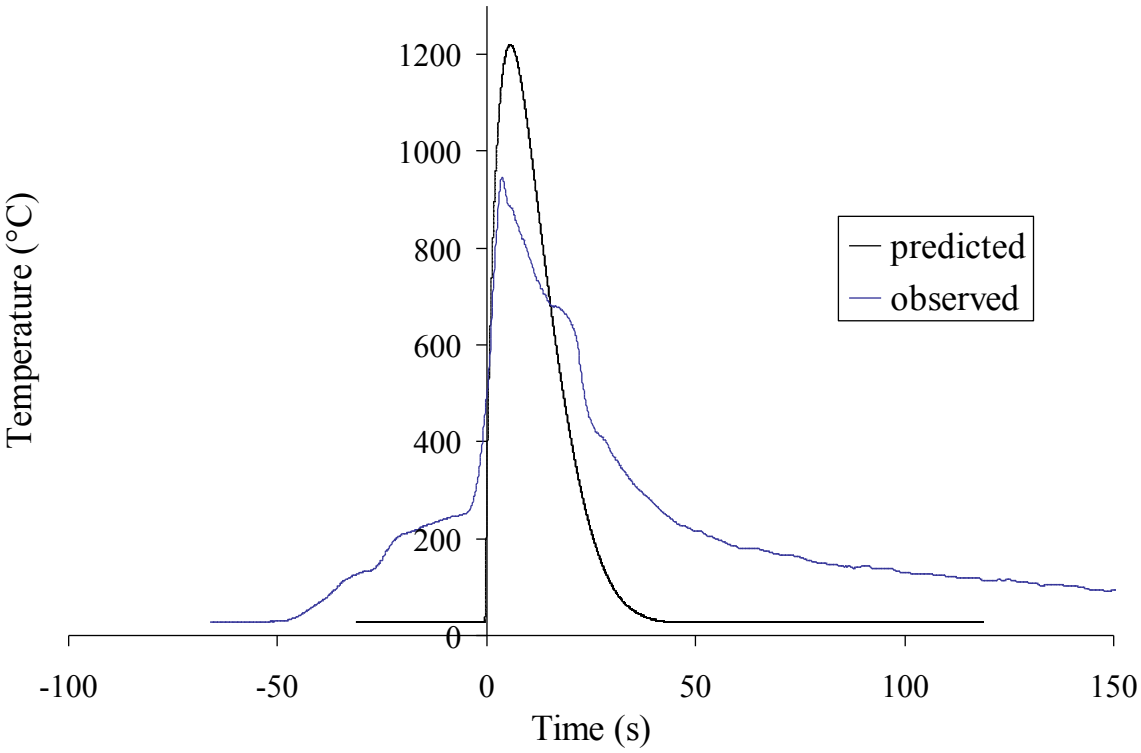

Figure 10: Experimental and predicted temperature curves for a 10° slope under 3 m s^{-1} wind condition

FIGURE CAPTIONS

Figure 1 *Schematic representation of the physical problem*

Figure 2.a *Flame tilt angle under slope condition*

Figure 2.b *Flame tilt angle under wind condition*

Figure 3 *Two dimensional reduction procedure*

Figure 4 *Experimental wind tunnel*

Figure 5 *Experimental and predicted temperature curves in slopeless and windless condition*

Figure 6 *Rates of spread of the radiative and the improved model for no slope under various wind conditions*

Figure 7 *Rates of spread of the radiative and the improved model for a slope of 5° under various wind conditions*

Figure 8 *Rates of spread of the radiative and the improved model for a slope of 10° under various wind conditions*

Figure 9 *Rates of spread of the improved model including a wind profile for no slope and under various wind conditions*

Figure 10 *Experimental and predicted temperature curves for a 10° slope under 3 m* s^{-1} *wind condition*